

MASS AND ISOTOPIC YIELDS FOR THE REACTION  
 $^{245}\text{CM}(\text{N}_{\text{TH}},\text{F})$  MEASURED AT LOHENGRIN

D. ROCHMAN

*Institut Laue Langevin, 6 rue Jules Horowitz, BP 156, 38042 Grenoble France*  
✉  
*CEA Cadarache, 13108 St Paul lez Durance Cedex France, rochman@ill.fr*

H. FAUST AND I. TSEKHANOVICH

*Institut Laue Langevin, 6 rue Jules Horowitz, BP 156, 38042 Grenoble France*  
*faust@ill.fr, tsekhanov@ill.fr*

S. OBERSTEDT

*IRMM Geel, Belgium, obst@irmm.jrc.be*

V. SOKOLOV

*PNPI Gatchina, Russia, vsokolo@hep486.pnpi.spb.ru*

F. GÖNNENWEIN

*Universität Tübingen, Germany, friedrich.goennenwein@uni-tuebingen.de*

F. STORRER

*CEA Cadarache, France, storrer@drncad.cea.fr*

F. HAAS

*IReS Strasbourg, France, Florent.Haas@IReS.in2p3.fr*

The fission fragment mass, charge, and kinetic energy distributions for the thermal neutron induced fission of  $^{245}\text{Cm}$  were measured using the LOHENGRIN mass separator at ILL Grenoble associated with a big ionization chamber ( $Z$ -identification) with a split anode (energy loss- remaining energy simultaneously measured,  $\Delta E - E_R$  technique). The ionization chamber was combined with a passive absorber (Stack of Parylene C foils) to further improve the  $Z$ -resolution for heavier products ( $A > 96$ ) up to 4 nuclear charges per mass. Considering the available experimental data prior to this work, the range of measured mass yields was extended from  $A = 76$ -132 to  $A = 67$ -167, and isotopic yields from  $A = 76$ -96 to  $A = 67$ -119, i.e. for corresponding nuclear charges ranging from  $Z = 26$  to 48. A comparison of these new data with the existing evaluations of fission product yields (JEF2.2 and ENDF/B-VI) and systematics (by Wahl) was also performed. A study of the global odd-even effect for protons was done and the results were compared with the data for the fission of other transuranium elements. The global  $\delta_Z$  value of proton odd-even effect calculated is  $10.5 \pm 0.5 \%$ , which fits well to the known systematics for the  $\delta_Z$  as a function of the fissility.

## 1 Introduction

Recently, a new specific interest for fission yields of "minor" actinides arose from R&D programs in France dealing with the management of long-lived nuclear waste. In this framework, the research is devoted at CEA (Commissariat à l'Énergie Atomique, France) to study the capabilities of new nuclear technologies to :

- limit the build-up of waste,
- ensure the safety of long term storage of waste
- separate the more radiotoxic isotopes by means of advanced spent fuel reprocessing so as to transmute (recycle) them afterwards using innovative reactor concepts and nuclear fuels.

Apart from the plutonium isotopes which are dominating the potential source of long term radiotoxicity among the transuranium elements produced in a nuclear power park of Pressurised Water Reactors (PWRs) loaded with standard uranium oxide fuels, the Curium (especially  $^{245}\text{Cm}$ ) and Americium (especially  $^{241}\text{Am}$ ) nuclides are the major radiotoxic ones with the cooling times up to  $10^5$  years. The  $^{245}\text{Cm}$  is therefore a candidate for transmutation research. In this context, the investigation of the reaction  $^{245}\text{Cm}(n_{th}, f)$  at the mass spectrometer Lohengrin has been done.

Unfortunately the data basis for  $^{245}\text{Cm}$  is scarce. Several experimental efforts for measuring yields in the thermal neutron induced fission of  $^{245}\text{Cm}$  have been made in the last years. Whereas the situation concerning chain yields was adequate for the light peak of the distribution, a pronounced deficit existed concerning the independent yields of single nuclides for masses above  $A = 94$ . Earlier data presented only isolated values, like the independent yields of the nuclides  $^{86}\text{Rb}$  and  $^{136}\text{Xe}$  <sup>2</sup> and the fractional cumulative yields of  $^{135}\text{I}$  and  $^{140}\text{Ba}$  <sup>3</sup> as well as the fractional independent yields of  $^{135}\text{Xe}$  <sup>4</sup>. Reference <sup>5</sup> provides 12 fractional cumulative yield values.

A few recent measurements <sup>1</sup> performed at the Lohengrin mass separator provides accurate values for the nuclear charge distribution from  $A = 76$  to 94 using a ionization chamber with a split anode. A new technique using an ionization chamber associated with a passive absorber has been used which allows a very powerful means to measure the isotopic yields from  $Z = 26$  up to  $Z = 48$ . Moreover, mass and kinetic energy distributions from  $A = 67$  up to  $A = 85$  and from  $A = 130$  up to  $A = 167$  have also been investigated.

## 2 Experimental Setup

The initial target material which originated from PNPI in Gatchina, Russia, had been produced with an isotopic composition of 9 % for  $^{244}\text{Cm}$  and 91 % for  $^{245}\text{Cm}$ . After chemical purification of the material, targets were fabricated at the Institut für Kernchemie, Mainz (Germany), by electrodeposition of curium in a form of  $\text{Cm}_2\text{O}_3$  onto a titanium foil (diameter 3 cm, thickness 50  $\mu\text{m}$ ) as circular spots (diameter 4 mm). The fission cross sections of  $^{244}\text{Cm}$  and of  $^{245}\text{Cm}$  for thermal neutrons are approximately 1.2 and 2100 barns, respectively. This determines a negligible contribution of the first isotope ( $^{244}\text{Cm}$ ) to the total activity measured in experiment (if compared to that one of  $^{245}\text{Cm}$ ). Further isotopes ( $^{240,241}\text{Pu}$ ), resulting from the  $\alpha$ -decay of the initial material, are produced only in tiny fractions and their contributions to the total activity could be neglected as well. Finally,  $^{246}\text{Cm}$  being produced quite abundantly in breeding reaction from  $^{245}\text{Cm}$ , has very small fission and neutron capture cross sections (0.2 and 1.2 barns respectively). Thus, all fission fragments measured in experiments had their origin in the Curium 245 isotope.

All experiments were performed at the mass spectrometer Lohengrin of the "Institut Laue Langevin" (ILL) Grenoble, France. This mass separator for unslowed fission products <sup>6</sup> consists of a condenser and a main magnet, and is installed at the high flux reactor providing a flux of  $5.10^{14} \text{ n.s}^{-1} \text{ cm}^{-2}$ . This device makes use of the electric and magnetic deflection fields to separate fission products according to their mass number  $A$ , their kinetic energy  $E_{kin}$  and their ionic charge number  $q$ . Fission fragments are selected according to the ratios mass over ionic charge ( $A/q$ ) and kinetic energy over ionic charge ( $E_{kin}/q$ ). To increase the luminosity and to decrease background, a second magnet <sup>7</sup> (RED magnet for Reverse Energy Dispersive) has been added at the exit of the spectrometer. With the RED magnet using 40 cm of the exit slit of the mass separator, an increase by a factor of 7 in the count rate can be achieved with as final detector an ionization chamber <sup>8</sup>, Fig. 1.

This chamber (filled with isobutane gas) is located at the exit of the RED magnet, just after the absorber foils.

## 3 Measuring technique

The usual manner to use the chamber is without the external absorber labelled number (7) on the figure 1, used in  $(\Delta E - E)$  mode. When a fragment enters the chamber, the sum of the signals from the two anodes is proportional

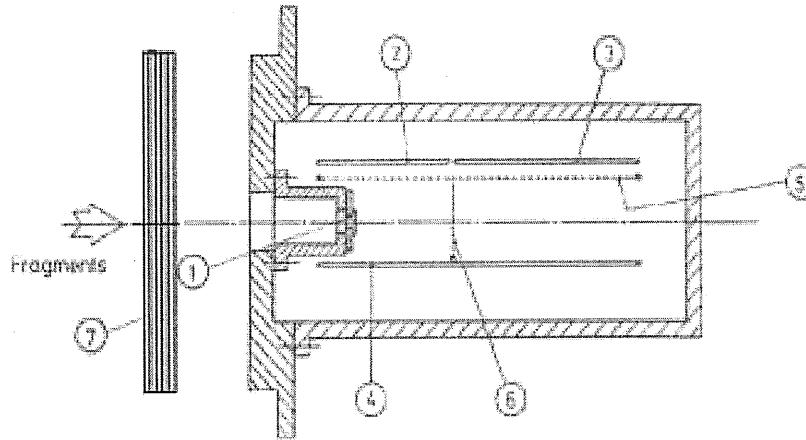


Figure 1. Schematic view of the ionization chamber : 1) entrance window, 2)  $\Delta E$  part of the anode, 3)  $E_{rest}$  part of the anode, 4) cathode, 5) Frisch grid, 6) separation grid between  $\Delta E$  and  $E_{rest}$  area, 7) stack of absorber foils

to the total kinetic energy of the fragment. In the case of a configuration  $(A, E_{kin}, q)$ , the mass  $A$  selected with ionic charge  $q$  and kinetic energy  $E_{kin}$ , will contain several nuclear charges  $Z_i, Z_{i+1}, \dots$ , which intensities should be defined. The deposited energy  $dE$  per unit of length  $dx$  for a fission fragment in an absorber is given by a function of the nuclear charge of the fragment, its mass and its kinetic energy (Bragg curve  $dE/dx$ ). The nuclear charge  $Z$  separation is feasible as long as the deposit energy  $\Delta E$ , function of the fragment mass  $A$  and the fragment nuclear charge  $Z_i$ , is quite different than  $\Delta E'$ , function of the fragment mass  $A$  and the fragment nuclear charge  $Z_{i+1}$ . This energy gap between to successive nuclear charge depends directly on the characteristics of the absorber (solid or gaseous) and of the fragments. This technique using a part of the gas of the chamber as in the  $(\Delta E - E)$  mode was successfully used until now and allowed the isotope separation up to the nuclear charge  $Z = 39$  (Y) <sup>1</sup>. But for higher  $Z$ , the Bragg curves show that for the two successive  $Z$ , the difference in the energy loss disappears in any gas as again verified experimentally in this work. In light of this limitation, a different method has been used to measure eight more nuclear charges. It is known from <sup>8</sup> that solid absorbers have better separation powers than gaseous

ones. So a solid absorber was added before the chamber. The solid absorber used here is a stack of 12 Parylen C foils of a thickness of  $0.58 \mu\text{m}$  ( $\pm 10\%$ ) each. The difference to the previous set up is that the absorber is placed outside the ionization chamber and hence a specific energy loss cannot be measured. The only observable is then the  $E_{rest}$  energy. It was measured with the ionization chamber being switched to the  $(\Delta E - E)$  mode. The energy left in the absorber will be different for different nuclear charges and the fragments no longer have the same energy when they penetrate into the chamber. Hence, the charge signal of the residual kinetic energy carries the information on nuclear charge.

#### 4 Results

Six targets with amount of  $^{245}\text{Cm}$  ranging from 12 to  $16 \mu\text{g}$  have been irradiated in a thermal neutron flux of  $5.10^{14} \text{ n.s}^{-1}.\text{cm}^{-2}$  during 10 days each. The targets were covered with a nickel foil of  $0.25 \mu\text{m}$  to avoid the sputtering and therefore uncontrolled loss of the target material. Mass yields have been determined from  $A = 67$  up to 85 and from  $A = 130$  up to  $167^a$ : at the mean kinetic energy  $\bar{E}_{kin}$  the ionic charge distribution is measured with  $(A, \bar{E}_{kin}, q_{i=1..8})$  and at the mean ionic charge  $\bar{q}$  the kinetic energy distribution is measured with  $(A, E_{i=1..8}, \bar{q})$ . Mass yields have been obtained by integration of previous distributions. Isotopic distributions have been determined with the absorber foils from mass 67 up to 85 and from 90 up to  $119^b$  for different kinetic energies at one or two ionic charge states (only few  $(A, E_{kin}, q_i)$  configurations provide only one mass; by changing the  $q$  value, the intensity of contaminations by other masses are increasing or decreasing). Isotopic yields  $Y(A, Z, q)$  have been obtained by integration of energy distribution for one ionic charge  $q_i$  and then, the average value of  $Y(A, Z, q_i)$  over  $q$  provides  $Y(A, Z)^9$ .

The Fig. 2 presents the kinetic energy for each fission fragments and the total kinetic energy.

As the fragment kinetic energy, the fragment ionic charge is a parameter of the spectrometer. The Fig. 3 presents the mean ionic charges  $\bar{q}$  and the standard deviation  $\sigma_q$  for all the measurements. We have observed some strong influence of internal conversion effects which enhance the charge state by two units, specially in the heavy peak for  $A = 144, 149, 151, 153, 155$  and 157. For the masses higher than 165 and lower than 70, the ionic charge

<sup>a</sup>mass yields from the mass 85 up to the mass 130 have been already measured by <sup>1</sup>

<sup>b</sup>isotopic yields from the mass 85 up to the mass 90 have been already measured by <sup>1</sup>

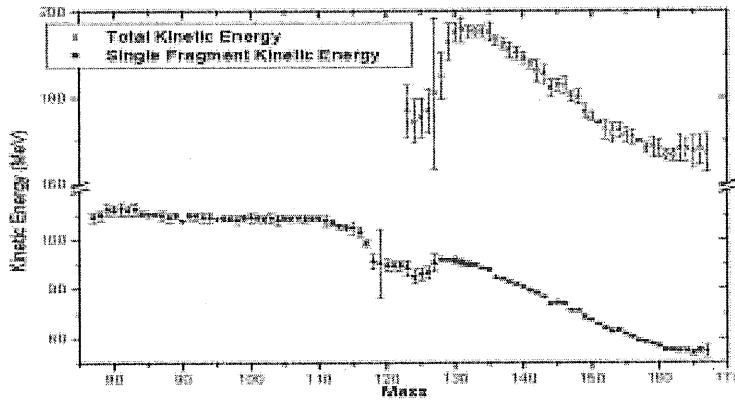


Figure 2. Fragments kinetic energy and total kinetic energy from the mass 67 up to 167

distribution is kept constant and equal to the value for previous mass because of the low statistics.

The Fig. 4, 5 and 6 present the measured mass and isotopic yields.

Thanks to the quality of the Parylen C absorber, it was possible to separate four or five nuclear charges inside one mass. The limit of this method appears when the deposit energies for two successive nuclear charges are equal or very near. Some calculations and measurements<sup>9</sup> show that the Parylen C separation power is decreasing when the kinetic energy is decreasing and when the nuclear charge is increasing. Because of this two limitations, the limit of the separation appears for the mass 119 which corresponds to the nuclear charge  $Z = 48$  (Cd).

## 5 Analysis

Thanks to the very good behaviour of Lohengrin and to the quality of the curium targets, it was possible to measure absolute yields down to  $10^{-6}\%$  with small uncertainties. The isotopic distribution is now known for the whole light peak from the very far asymmetric fission to the symmetry region.

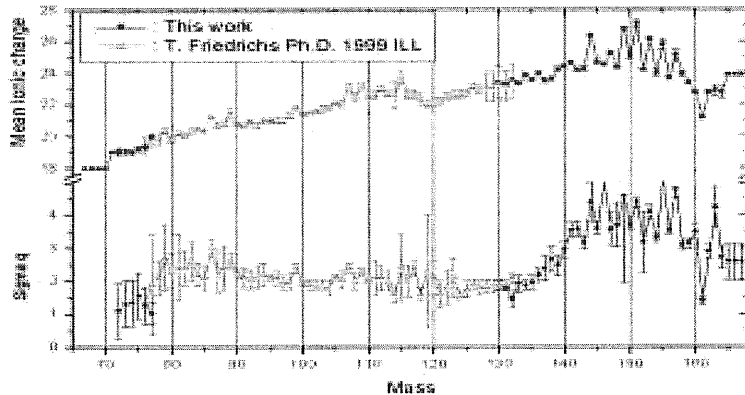


Figure 3. Mean ionic charge  $\bar{q}$  and  $\sigma_q$  from the mass 67 up to 167

For the first time, the heavy mass region was investigated. These measurements show the possibility to determine complete isotopic distribution until cadmium and complete mass distribution for other actinides.

To evaluate the new yields contribution to evaluated data, comparisons have been done with the data in libraries JEF2 and ENDF/BVI and with the Wahl systematics<sup>9</sup>. In the maxima of the mass yield region, some differences already exist between the libraries and between the libraries and Wahl yields. Whereas the yields in the Wahl systematics are smooth, strong peaks appear in the libraries data for the masses 139, 137 and 107 for JEF2 and the mass 136 for ENDF/BVI. These peaks are not seen in our measurements.

A strong difference appears in the symmetry region where the evaluated data from libraries are a factor 10 under measured yields. This difference comes from the fact that the libraries used previous measurements<sup>(2 and 5)</sup> which are underestimated. In the very asymmetric fission, new measurements show enhanced yields around the mass 70. This phenomena is not present in the libraries: JEF2 shows a constant mass yield decreasing with the same order of magnitude than Lohengrin measurement, and ENDF/BVI underestimates the yields in the region by a factor ten.

With the total isotopic distribution in the light peak, it is now possible to

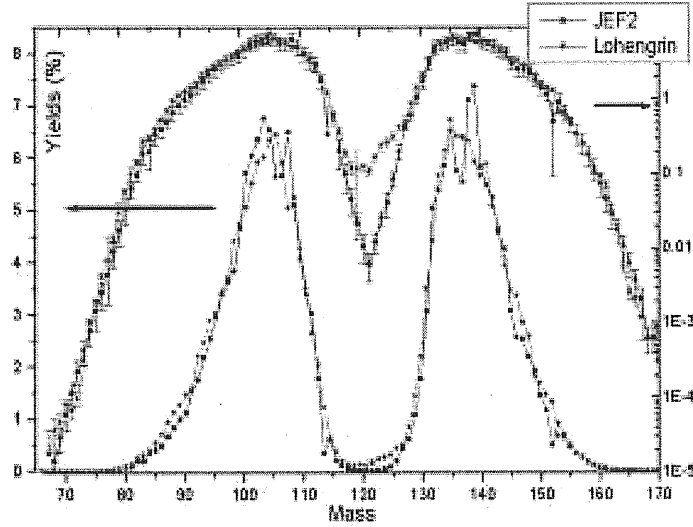


Figure 4. Mass yields from the reaction  $^{245}\text{Cm}(n_{th}, f)$ . The full dots are from the JEF2 libraries and the open dots are from the Lohengrin measurements

calculate the total proton odd-even effect with the function (1) :

$$\delta_Z = \frac{Y_e - Y_o}{Y_e + Y_o} \quad (1)$$

with  $Y_{e-(o)}$  the sum over all the even (odd) charge yields. The calculated value amounts to  $10.5 \pm 0.5\%$  and is plotted in function of the fissility parameter with the values from other actinides on Fig. 7.

This new value for the  $^{245}\text{Cm}$  is in good agreement with the known systematics and shows that the excitation energy of the nucleus is increasing with the fissility parameter. A simple formula allows to calculate the excitation energy at the scission point <sup>10</sup> :

$$E_x(\text{MeV}) = -4ln(\delta_Z) \quad (2)$$



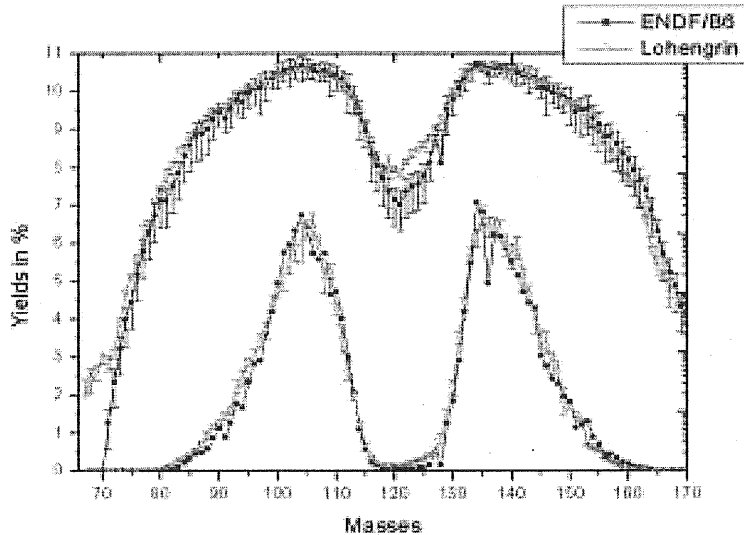


Figure 5. Mass yields from the reaction  $^{245}\text{Cm}(n_{th}, f)$ . The full dots are from the ENDF/B6 libraries and the open dots are from the Lohengrin measurements

For the curium 245, the excitation energy thus calculated is 9 MeV. As for the other fissile actinides <sup>11</sup>, this energy is equal to 30 % to the total energy released between the saddle point and the scission point.

## 6 Conclusions and perspective

These new measurements on the Lohengrin mass spectrometer provide a complete set of data for the mass yields in the very far asymmetric fission from  $A = 67$  up to  $A = 167$ . Thanks to the measurement using a passive absorber associated with the big ionization chamber, the isotopic yields are now known for the light peak mass distribution up to the symmetry region. The comparisons with libraries and systematics data confirm the data

improvement due to the high mass and charge resolution of the Lohengrin mass spectrometer. It would be very interesting to systematically apply this stacked foils technique at Lohengrin to further investigate the fission fragment mass, charge and kinetic energy distributions of other actinides (starting with uranium or plutonium fissile systems).

Furthermore, the development of gamma, beta and delayed-neutron spectroscopy of the separated fission products is under investigation at Lohengrin so as to provide key data for reactor physics purposes (decay heat prediction, reactor kinetics, etc...).

## 7 Acknowledgements

We wish to thank Prof. H. O. Denschlag from the Johannes-Gutenberg Universität, Institut für Kernchemie, Mainz (Germany), for his collaboration on the stage of the target preparation and for his time spent in scientific discussions.

## References

1. T. Friedrichs, Untersuchung der neutroneninduzierten Spaltung von Curium 245 and Plutonium 241, Ph.D. thesis, Technischen Universität Carolo-Wilhelmina, Braunschweig, 1998
2. H.R. Von Gunten, Flynn, Glendenin, Distribution of mass and charge in the fission of  $^{245}\text{Cm}$ , Physical Reviews, 161, 1192-1195 (1967)
3. T. Datta et al., Charge Distribution in the thermal neutron fission of  $^{245}\text{Cm}$  : fractional cumulative yields of  $^{135}\text{I}$  and  $^{140}\text{Ba}$ , Physical Review C, 21, 1411 (1980)
4. R. Harbour et al., Nuclear charge distribution in fission : fractional independent yields of  $^{135}\text{Xe}$  from thermal neutron induced fission of  $^{245}\text{Cm}$ , Physical Review C, 10, 769-773 (1974)
5. J. Dickens et al., Yields of fission products by thermal neutron fission of  $^{245}\text{Cm}$ , Physical Review C, 23, 331-350 (1981)
6. Schrader et al. Experiments with fission products at the Lohengrin mass separator, Kerntechnik, 19 January 1977.
7. G. Fioni et al. ; Reduction of energy dispersion on a parabola mass spectrometer, Nucl. Instr. Methods in Phys. Research A332, 175(1993)
8. U. Quade, A high resolution ionisation chamber tested with fission, Nucl. Inst. Meth., 164, p435, 1979
9. D. Rochman, Ph.D. thesis, ILL & CEA Cadarache, France, 2001

10. F. Gönnenwein., Mass Charge and Kinetic Energy in fission fragments, p287, The Nuclear Fission Process, Cyriel Wagemans, CRC Press, 1991
11. M. Asghar et al., Saddle to scission landscape in fission : experiments and theories, Journal de Physiques, Colloques 6, 1984, p.455

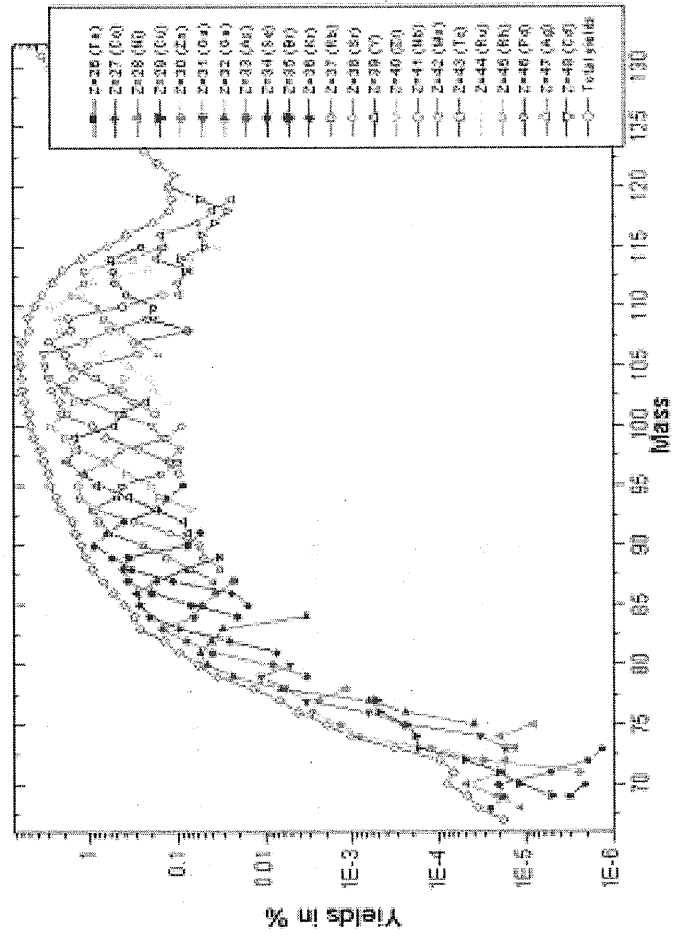


Figure 6. Isotopic yields for the reaction  $^{245}\text{Cm}(n_{th}, f)$ .

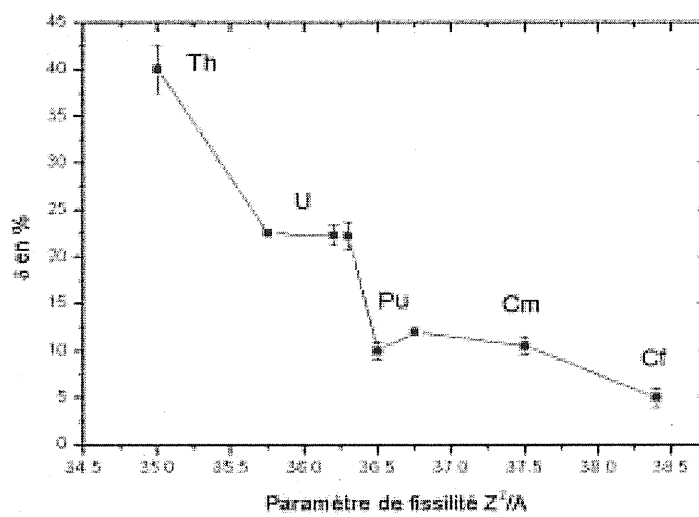


Figure 7. Global proton odd-even effects in function of the fissility parameter

